

<https://doi.org/10.33472/AFJBS.6.6.2024.6230-6249>



African Journal of Biological Sciences

Journal homepage: <http://www.afjbs.com>



Research Paper

Open Access

## Synthesis, In-Vitro and In-Silico Screening of Novel Oxadiazole Derivatives as Potent Anti-Mycobacterial Agents

Manjoor Ahamad Syed<sup>1</sup>, Pradeep Kumar M.R<sup>2\*</sup>, Kerryan Joseph A Dsilva<sup>3</sup>, Akshata P. Hebbali<sup>2</sup>

<sup>1</sup>Department of Pharmaceutical chemistry, Raghavendra Institute of Pharmaceutical Education and Research- Anantapuramy-515721, Andhra Pradesh

<sup>2</sup>Department of Pharmaceutical chemistry, KLE College of Pharmacy, Vidyanagar, Hubballi-580031. (A Constituent unit of KAHER, Belagavi) Karnataka.

<sup>3</sup>Department of Pharmaceutical chemistry, D.R.Karigowda College of Pharmacy, Kuvempunagar, Hassan-573201, Karnataka

\* **Corresponding Author:** Dr. Pradeep Kumar M.R [pradeepmrpk@yahoo.co.in](mailto:pradeepmrpk@yahoo.co.in)

### Article Info

Volume 6, Issue 6, June 2024

Received: 23 April 2024

Accepted: 31 May 2024

Published: 26 June 2024

[doi: 10.33472/AFJBS.6.6.2024.6230-6249](https://doi.org/10.33472/AFJBS.6.6.2024.6230-6249)

### ABSTRACT:

The current research is concerned with the synthesis of novel disubstituted oxadiazole derivatives and evaluation of their anti-tubercular activity by in-vitro and in-silico approach. The main goal of this work is to investigate and analyse the effectiveness, safety, and potential impact of these novel compounds in the treatment of tuberculosis. The titled compounds 3a-3h were synthesized by a 3 steps reaction, which were characterized by IR, <sup>1</sup>H NMR and Mass spectral data. These compounds were subjected to In-vitro studies and screened using MABA method by keeping isoniazid as the standard drug. Further, the In-silico studies were performed on Protein 6s9b, obtained from PDB RCSB. The in-vitro results showed that, compound 3a, 3b and 3c exhibited potent anti-tubercular activity with MIC value of 12.5 µgm/ml. The docking studies revealed that the compounds 3b, 3a and 3c with the values -7.3, -7.2 and -7.2 respectively, showed the highest binding affinity of the ligand-receptor at the target active site of the enzyme 6s9b. Additionally, all the compounds showed zero violation for drug likeliness parameter which predicts that these ligands obey Lipinski rule, and hence they are druggable.

**Keywords:** In-silico, Lipinski rule, MABA, Oxadiazole, Tuberculosis.

© 2024 Manjoor Ahamad Sued, This is an open access article under the CC BY license (<https://creativecommons.org/licenses/by/4.0/>), which permits unrestricted use, distribute on, and reproduction in any medium, provided you give appropriate credit to the original author(s) and the source, provide a link to the Creative Commons license, and indicate if changes were made

## 1. Introduction

Tuberculosis (TB) is the world's leading infectious disease threat(1). Almost a quarter of the global population is infected with *Mycobacterium tuberculosis*, putting millions at risk of tuberculosis (TB) illness. In the first 2-5 years following infection, 5-10% of people infected with *Mycobacterium TB* (*M. tuberculosis*) acquire the disease(2). According to the (World Health Organization [WHO], 2018), 1.7 billion people (23%) of the world's population are estimated to have latent tuberculosis (TB), indicating a risk of developing active TB over their lifetime (World Health Organization [WHO], 2018). Approximately 10.4 million cases of tuberculosis were reported worldwide, with 5 million (56%) men, 3.5 million (34%) women, and 1 million (10%) children (WHO, 2017)(3). It can affect anyone, but certain population groups are at a higher risk of getting TB infection and progressing to disease once infected; these groups include people living with HIV, health workers, and those in environments where *M. tuberculosis* transmission is high(4). Approximately 85% of those with tuberculosis can be successfully treated for six months with a drug scheme; treatment also has the added benefit of further limiting infection spread(1). TB is often diagnosed using the GeneXpert assay, sputum-smear microscopy, and chest radiography. However, the culture method is regarded as the gold standard for detecting the causative agent of tuberculosis, *Mycobacterium tuberculosis* (MTB), but it is a time-consuming diagnosis with substantial contamination risks(3). Despite the fact that the global number of TB deaths decreased by 42% between 2000 and 2017, and the yearly fall in global TB incidence rate is approximately 1.5%(1), much more work is required to speed progress towards global milestones to eradicate TB(5). The development of innovative antimycobacterial medications has been a significant milestone in TB control over the last 15 years(6) and understanding the host response to *M. tuberculosis* infection is a critical component of attempts to eradicate TB through the development of effective vaccines and immunological treatments(7).

Compounds with heterocyclic ring structures are highly significant in both medicine and industry among which Oxadiazole, being a heterocyclic compound is widely seen in drug-like molecules and frequently used in medication production due to its outstanding unique features(8). Oxadiazole is a heterocyclic aromatic compound containing one oxygen and two nitrogen atoms in a five membered ring(9). It occurs in various isomeric forms like 1,2,3-oxadiazole, 1,2,4-oxadiazole, 1,2,5-oxadiazole and 1,3,4-oxadiazole(10) as represented in Fig. 1(11). However, because of their numerous essential chemical and biological features, 1,3,4-oxadiazole is more known and investigated by researchers. Recently, it was discovered and reported that 1,3,4-oxadiazole derivatives with suitable substitutions at 2 and 5 positions demonstrated significant biological activities such as antibacterial(12,13), anticonvulsant(14), antitumor(15–20), anti-tubercular(13,21), anti-viral(22,23), antioxidant(8), anti-inflammatory(8,24–26), antihypertensive(27), analgesic(28). The disubstituted oxadiazole scaffolds containing marketed drugs are reported in Fig. 2(11). The urge to eradicate tuberculosis, emphasized the synthesis of 2, 5-disubstituted oxadiazole derivatives.

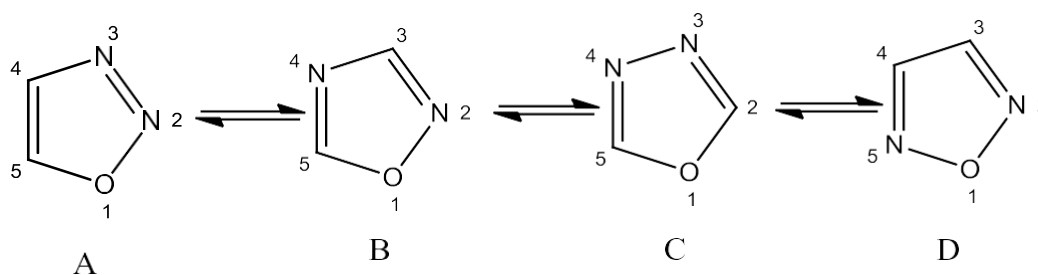


Fig. 1: 4 Isomeric forms of Oxadiazole heterocyclic ring

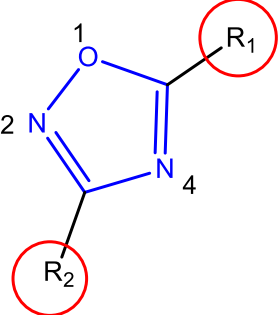
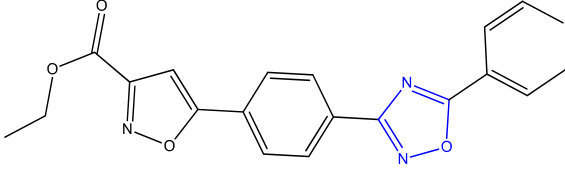
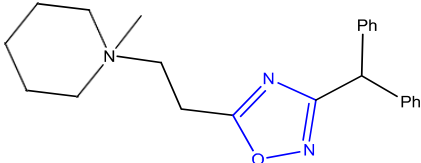
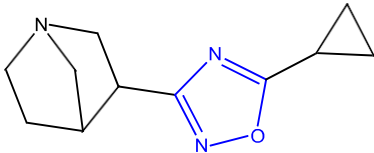
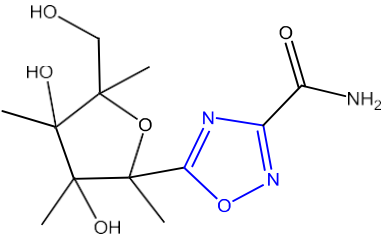
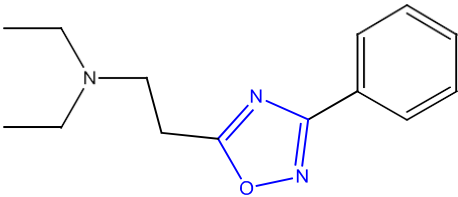
Disubstituted 1,2,4Oxadiazole	Bioactive Medications	Structures
	Anti-Tuberculosis	
	Antitussive Libexin	
	Antiglaucoma	
	Anticancer 5- Glycosyloxadiazol e	
	Analgesic Oxolamine	

Fig. 2: Some marketed medications containing Disubstituted Oxadiazole derivatives

## 2. Materials and methods

### Synthesis of 2-(4-substituted phenoxy) acetohydrazide

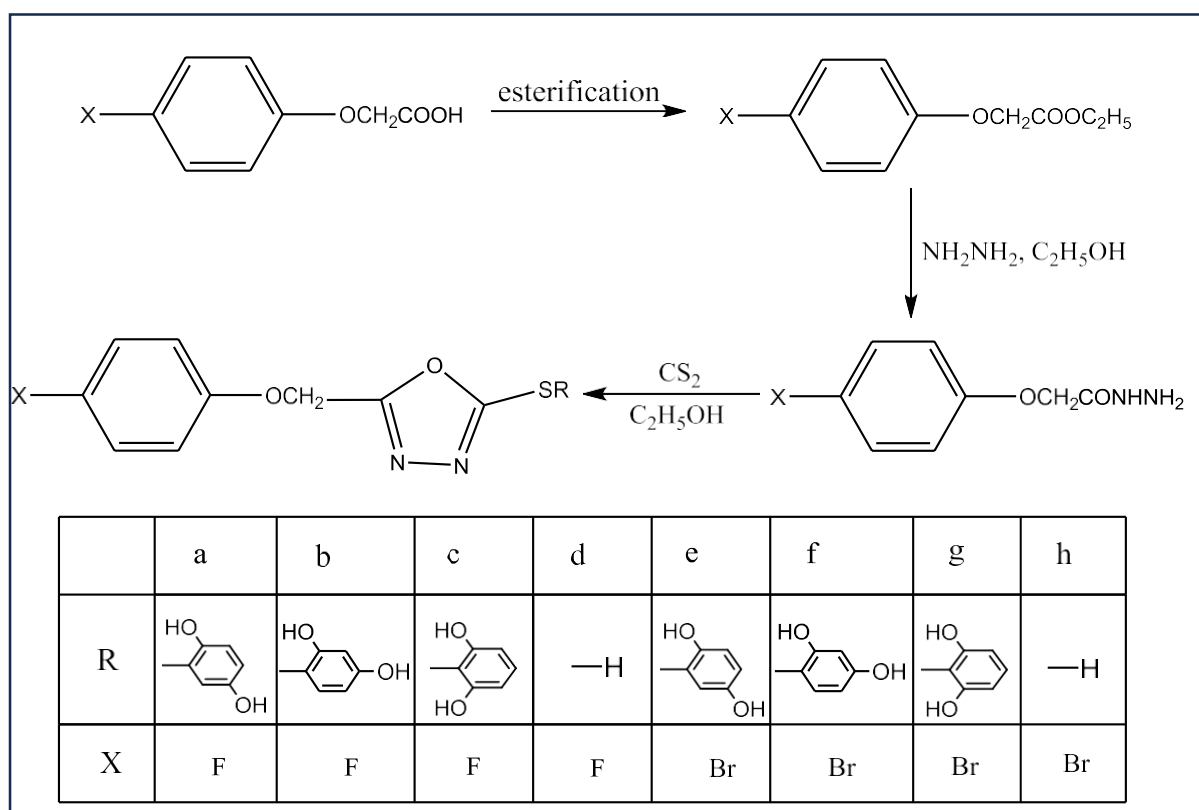
A mixture of ethyl (4-Substituted phenoxy) acetate (21.4g, 0.1 mol) and hydrazine hydrate (60.0 ml) in 90ml of ethanol was refluxed on water bath for 6 hr. The precipitate was filtered and recrystallised from ethanol. m.p.141°C<sup>7</sup>, yield 85%. IR (KBr): 3310 (NH<sub>2</sub>), 3210 (NH), 1622 (C=O), 2916 (Ar-CH).

## 5-[(4- Substituted phenoxy) methyl]-1,3,4-oxadiazole-2-thiol (3A &amp; 3H)

To a mixture of 2-(4- Substituted phenoxy)acetohydrazide (2.18 g, 0.01 mol) and ethanol (200 ml), a solution of KOH (0.84 g, 0.015 mol) in ethanol (20 ml) was added which was followed by the addition of carbon disulfide (20ml).The reaction mixture was refluxed for 8 hr, then concentrated and acidified with dil. hydrochloric acid. The resulting solid was collected, washed with water and recrystallised from ethanol. m.p.92 °C, yield 100%.

## 2-({5-[(4- Substituted phenoxy) methyl]-1,3,4-oxadiazole-2yl}sulfanyl)benzene-1,3-diol (3A, 3B, 3C, 3E, 3F &amp; 3G)

To a mixture of 5-[(4- Substituted phenoxy) methyl]-1,3,4-oxadiazole-2-thiol (1.04 g, 0.005 mol) and p-benzoquinone (0.54g, 0.005 mol), anhydrous xylene(2.5ml) was added. The reaction mixture was refluxed for 10 hr and xylene was removed under reduced pressure. The solid obtained was recrystallised from ethanol. m.p. 104 °C, yield 85%.

**In-vitro Activity**

Using the Microplate Alamar Blue test (MABA), the MIC values for the newly synthesized compounds against *M. tuberculosis* strain H37Rv were determined while isoniazid served as the reference medication. The 96-well plate was filled with 100 L of Middlebrook 7H9 broth, and serial dilutions of various substances at concentrations of 0.2, 0.4, 0.8, 1.6, 3.125, 6.25, 12.5, 25, 50, and 100 g/ml were made directly on the plate. Plates were covered and sealed with parafilm and incubated at 37°C for 5 days. Then, 25 ml of freshly prepared 1:1 mixture of alamar blue reagent and 10% Tween 80 was added to the plate and incubated for 24 hr. No bacterial growth was indicated by a well that was blue, whereas growth was shown by a well that was pink. The lowest drug concentration that prevented a colour change from blue to pink was known as the MIC.

All synthetic compounds' melting points were ascertained using a digital melting point equipment and are uncorrected. By using silica gel as a solvent solution together with n-hexane and ethyl acetate, TLC was used to check the purity of each component. On a Bruker spectrophotometer in KBr, IR spectra were obtained. The  $^1\text{H}$  NMR spectra were recorded on Bruker spectrophotometer 400 MHz instruments using  $\text{CDCl}_3/\text{DMSO}$  as the solvent and TMS as the internal standard; chemical shifts are given in ppm.

### 3. Results and discussion

Table 1: Anti-TB screening of compounds by MABA method.

Compound	MIC $\mu\text{gm/mL}$
3A	12.5
3B	12.5
3C	12.5
3D	>100
3E	>100
3F	100
3G	>100
3H	50
Isoniazid	0.25

Table 2: Binding affinity of the docked ligands.

ligands	Binding affinity	Rmsd/ub	Rmsd/lb
3B	-7.3	0	0
3A	-7.2	0	0
3C	-7.2	0	0
3E	-7.0	0	0
3F	-7.0	0	0
3G	-7.0	0	0
3D	-5.9	0	0
3H	-5.9	0	0

Table 3: Physicochemical properties of the docked ligands

Compounds	Formula	Molecular weight	TPSA	H-bond acceptors	H-bond donors
3A	$\text{C}_{15}\text{H}_{11}\text{FN}_2\text{O}_4\text{S}$	334.32 g/mol	113.91 $\text{A}^0$	7	2
3B	$\text{C}_{15}\text{H}_{11}\text{FN}_2\text{O}_4\text{S}$	334.32 g/mol	113.91 $\text{A}^0$	7	2
3C	$\text{C}_{15}\text{H}_{11}\text{FN}_2\text{O}_4\text{S}$	334.32 g/mol	113.91 $\text{A}^0$	7	2
3D	$\text{C}_9\text{H}_7\text{FN}_2\text{O}_2\text{S}$	226.23 g/mol	86.95 $\text{A}^0$	5	0
3E	$\text{C}_{15}\text{H}_{11}\text{BrN}_2\text{O}_4\text{S}$	395.23 g/mol	113.91 $\text{A}^0$	6	2
3F	$\text{C}_{15}\text{H}_{11}\text{BrN}_2\text{O}_4\text{S}$	395.23 g/mol	113.91 $\text{A}^0$	6	2
3G	$\text{C}_{15}\text{H}_{11}\text{BrN}_2\text{O}_4\text{S}$	395.23 g/mol	113.91 $\text{A}^0$	6	2
3H	$\text{C}_9\text{H}_7\text{BrN}_2\text{O}_2\text{S}$	287.13 g/mol	86.95 $\text{A}^0$	4	0

Table 4: Lipophilicity and Drug Likeliness of the Selected Ligands

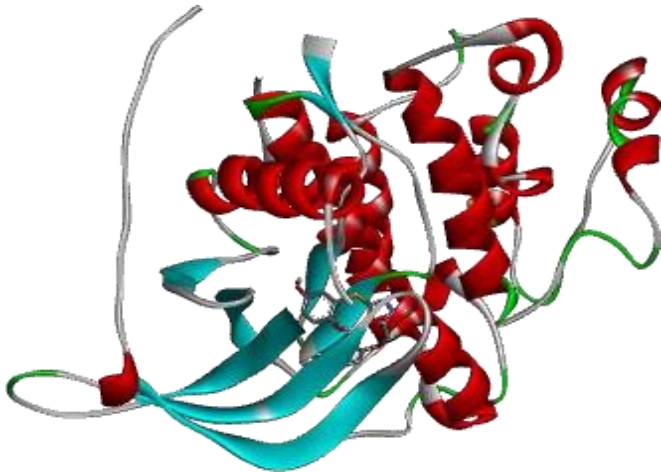
Compounds	Lipophilicity			Drug Likeliness	
	$\log P_{o/w}(\text{XLOGP3})$	$\log P_{o/w}(\text{WLOG})$	$\log P_{o/w}(\text{MLOGP})$	lipinski	Veber
3A	3.04	3.62	2.07	Yes;0 violation	Yes

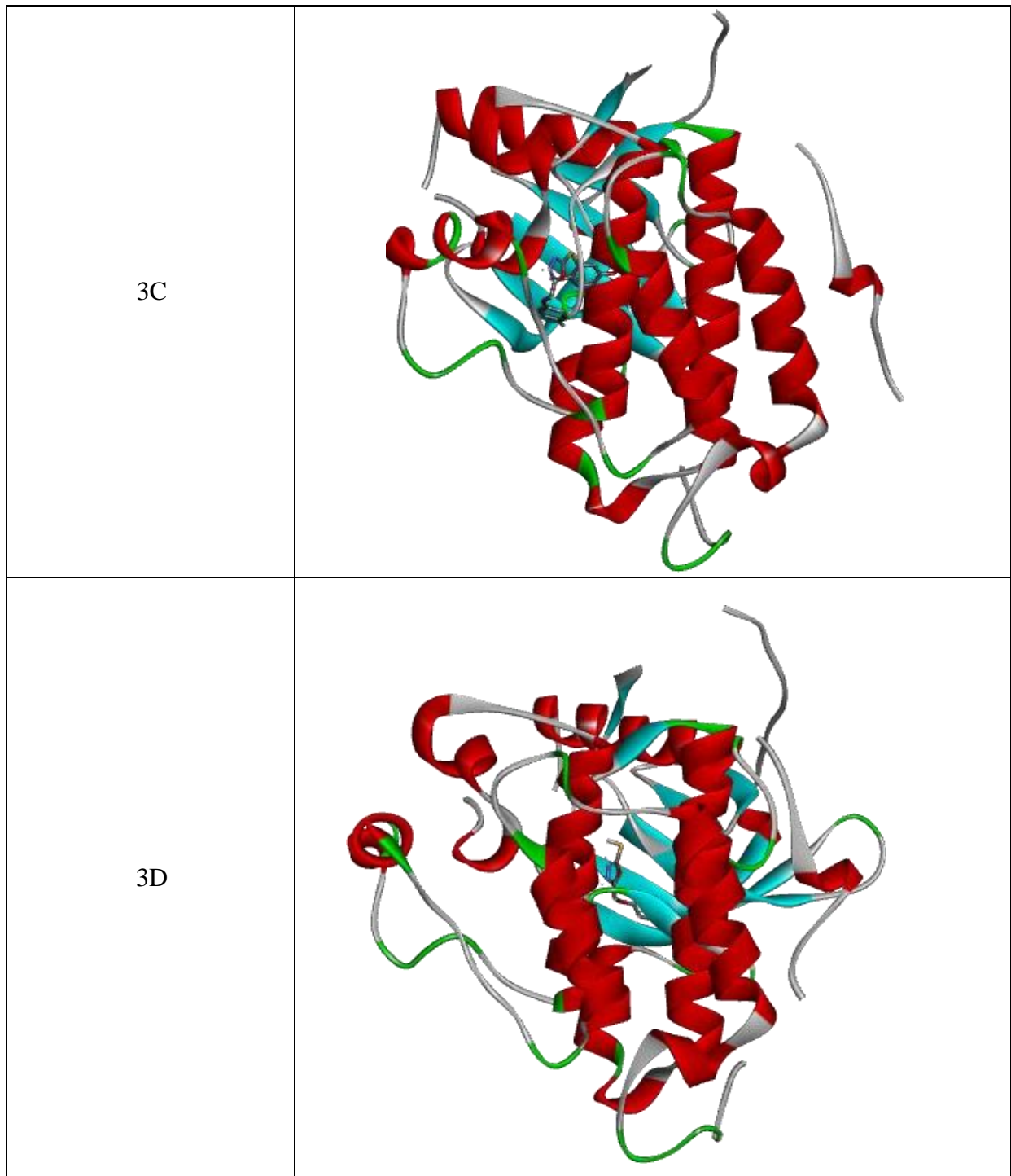
3B	3.04	3.62	2.07	Yes;0 violation	Yes
3C	3.04	3.62	2.07	Yes;0 violation	Yes
3D	1.84	2.34	1.50	Yes;0 violation	Yes
3E	3.63	3.82	2.31	Yes;0 violation	Yes
3F	3.63	3.82	2.31	Yes;0 violation	Yes
3G	3.63	3.82	2.31	Yes;0 violation	Yes
3H	2.43	2.55	1.80	Yes;0 violation	Yes

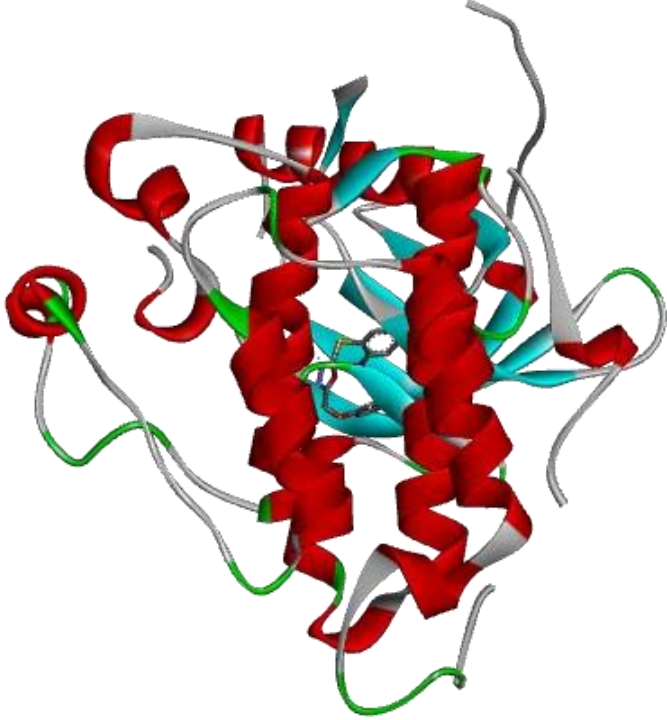
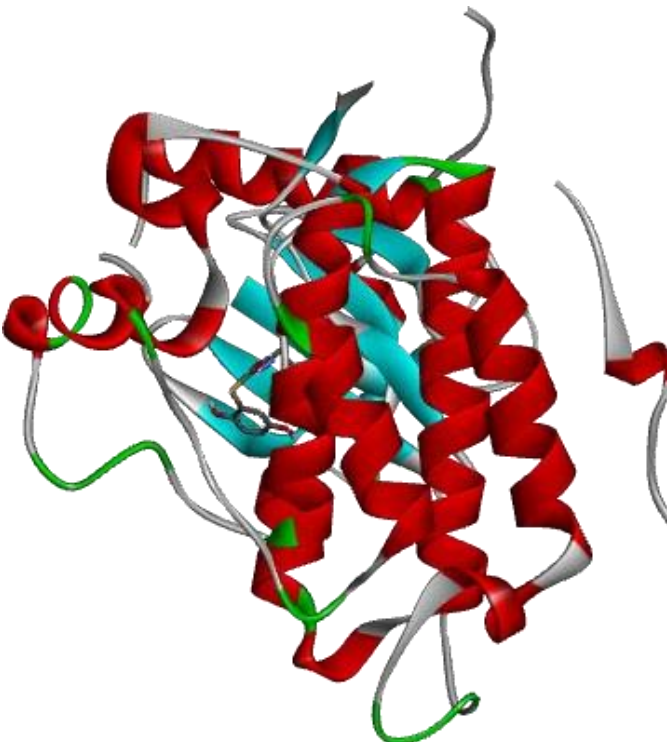
Table 5: Pharmacokinetics of the Docked Ligands

Compounds	Pharmacokinetics					
	GI absorption	BBB permeant	P-gp substrate	CYP2D6 inhibitor	CYP3A4 inhibitor	Log K <sub>p</sub> (skin permeation)
3A	High	No	No	Yes	Yes	-6.18 cm/s
3B	High	No	No	Yes	Yes	-6.18 cm/s
3C	High	No	No	Yes	Yes	-6.18 cm/s
3D	High	No	No	No	No	-6.37 cm/s
3E	High	No	No	No	Yes	-6.13 cm/s
3F	High	No	No	No	Yes	-6.13 cm/s
3G	High	No	No	No	Yes	-6.13 cm/s
3H	High	No	No	No	No	-6.33 cm/s

Table 6: 3D Structures of the Docked Ligands

Ligands	3DStructures
3A	



<p>3E</p>	 A 3D ribbon diagram of a protein structure labeled 3E. The protein is shown in a complex, multi-domain fold. The main body of the protein is colored red, with several loops and helices extending outwards. A prominent cyan-colored helix is visible in the center. A green-colored loop is located on the left side. The overall structure is compact and globular.
<p>3F</p>	 A 3D ribbon diagram of a protein structure labeled 3F. The protein is shown in a complex, multi-domain fold, similar to 3E. The main body of the protein is colored red, with several loops and helices extending outwards. A prominent cyan-colored helix is visible in the center. A green-colored loop is located on the left side. The overall structure is compact and globular.



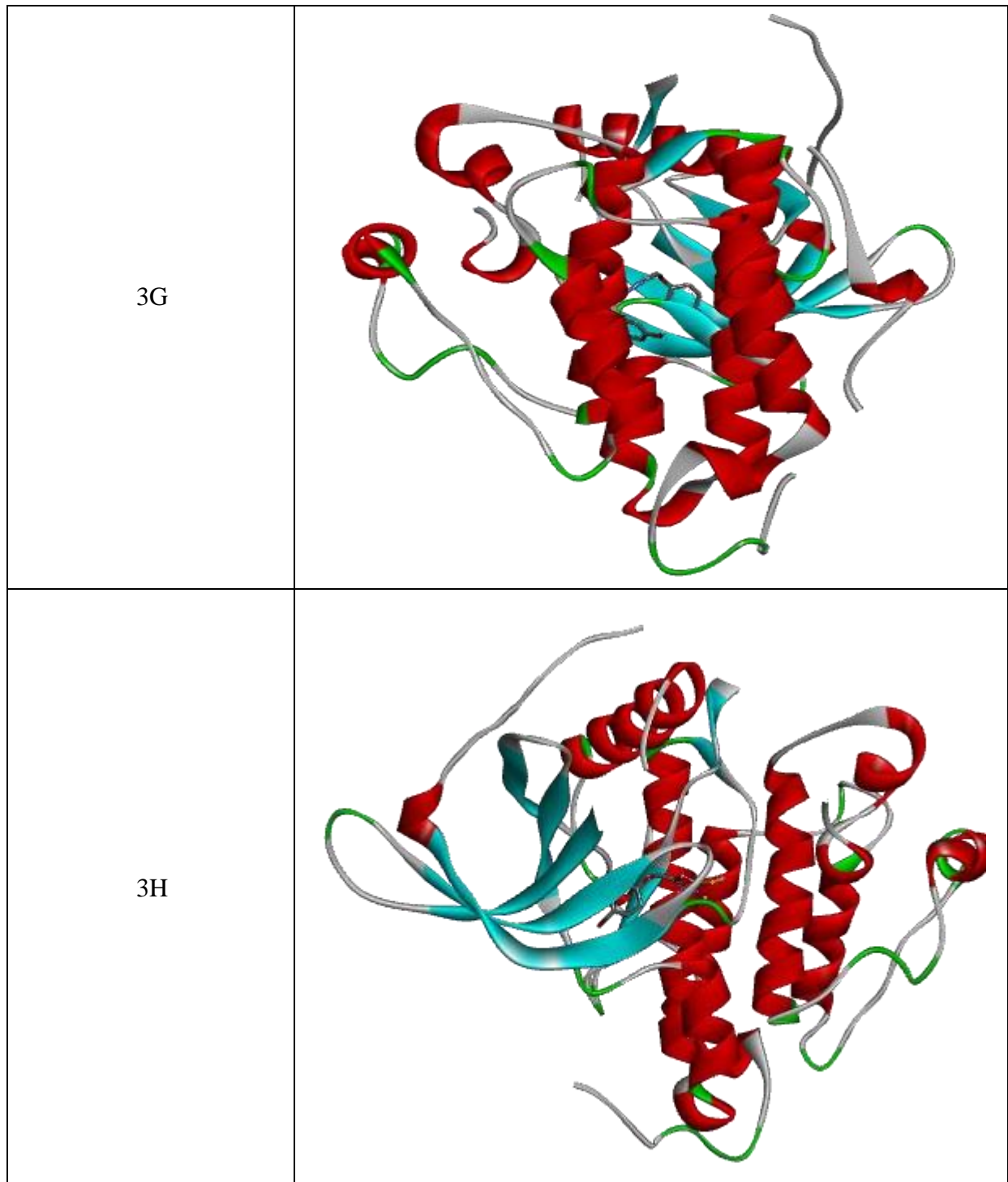
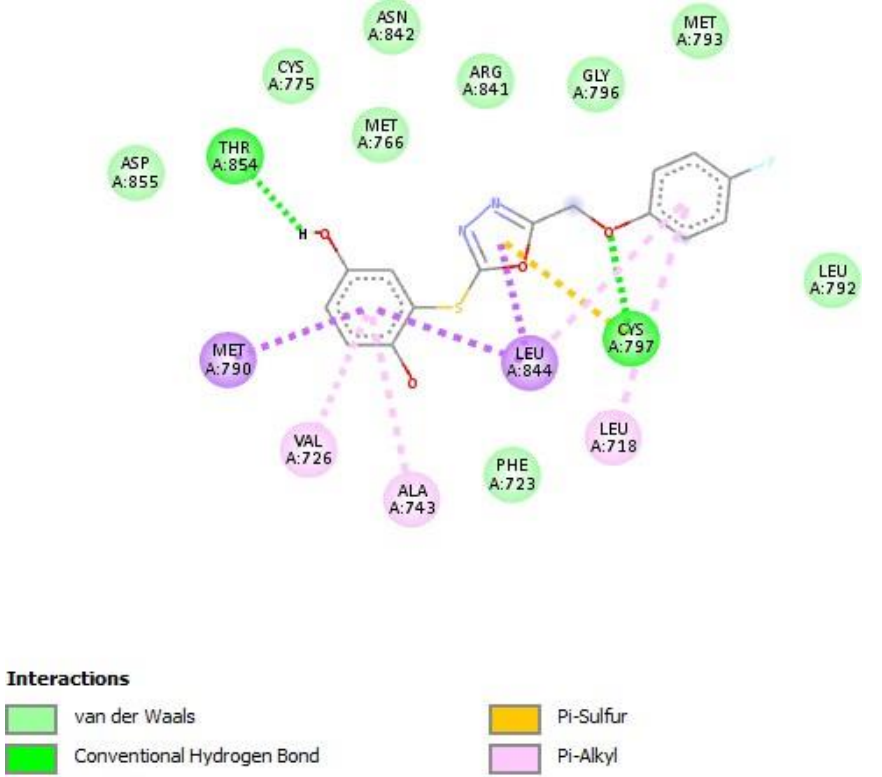
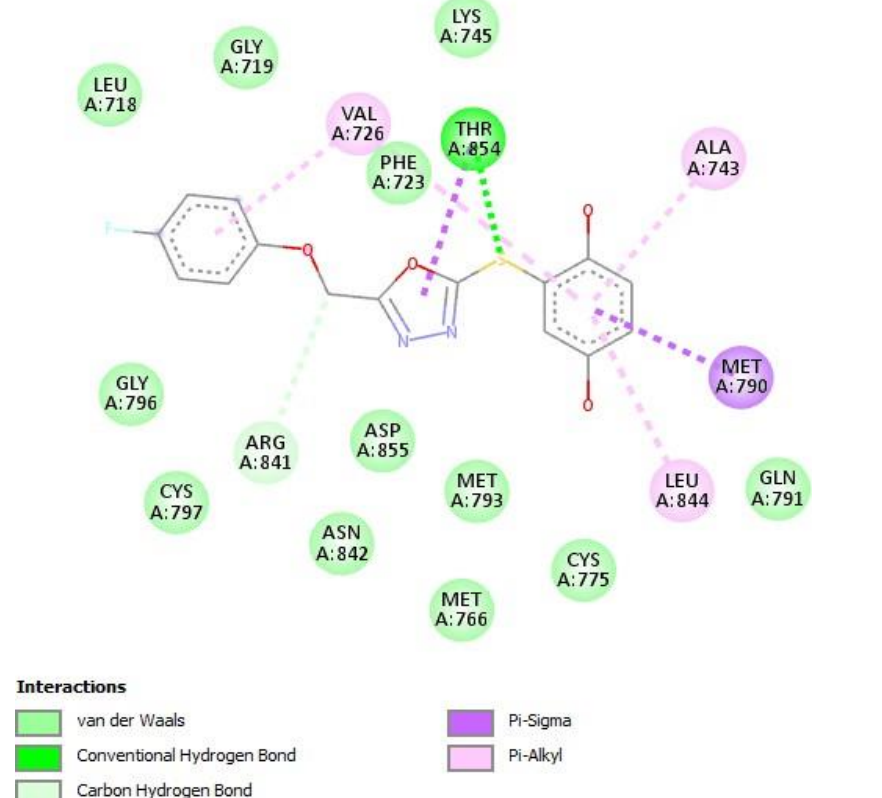
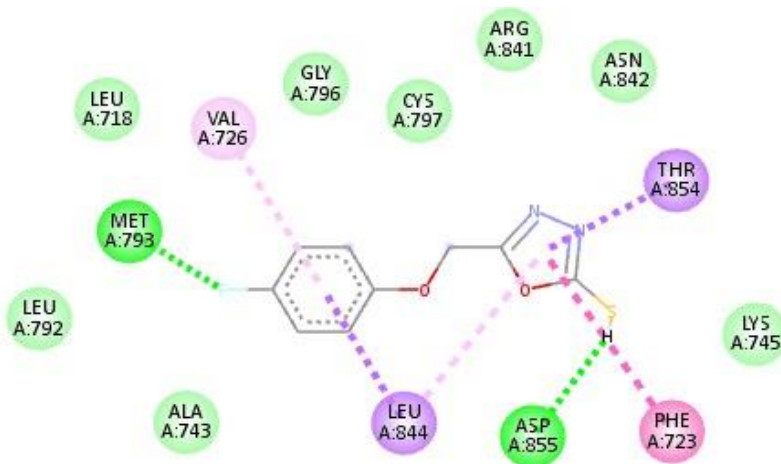


Table 7: The 2D Structures of the Docked Ligands

Ligands	2D Structures
3A	 <p><b>Interactions</b></p> <ul style="list-style-type: none"> <li>van der Waals</li> <li>Conventional Hydrogen Bond</li> <li>Pi-Sulfur</li> <li>Pi-Alkyl</li> <li>Pi-Sigma</li> </ul>
3C	 <p><b>Interactions</b></p> <ul style="list-style-type: none"> <li>van der Waals</li> <li>Conventional Hydrogen Bond</li> <li>Carbon Hydrogen Bond</li> <li>Pi-Sigma</li> <li>Pi-Alkyl</li> </ul>

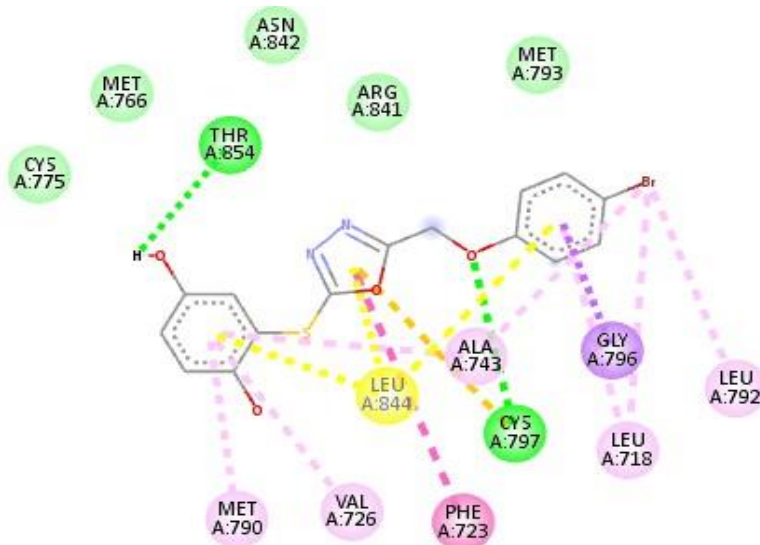
3D



**Interactions**

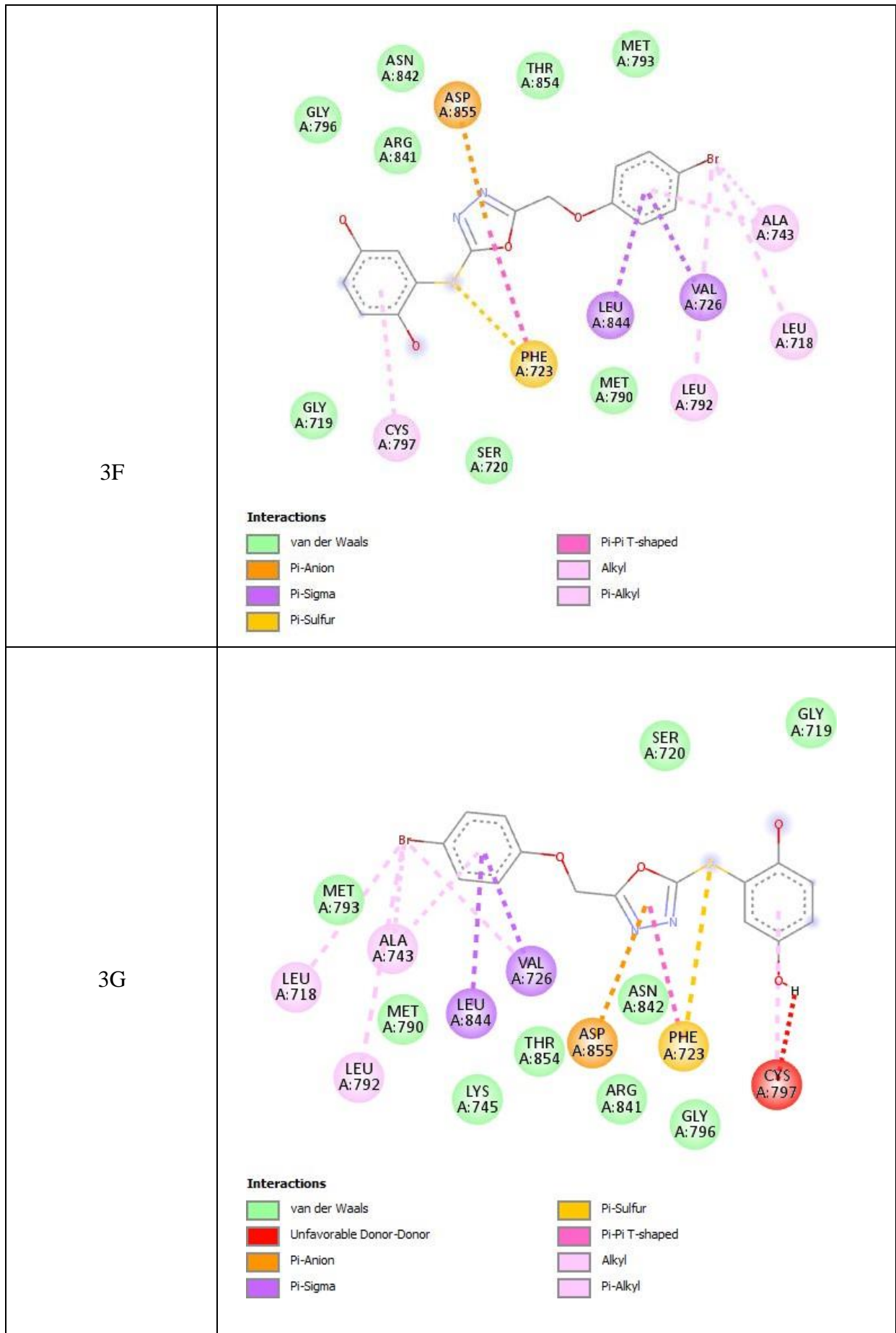
- |   |   |
|---|---|
| <span style="display:inline-block; width:15px; height:15px; background-color:#90EE90; border:1px solid black;"></span> van der Waals              | <span style="display:inline-block; width:15px; height:15px; background-color:#800080; border:1px solid black;"></span> Pi-Sigma       |
| <span style="display:inline-block; width:15px; height:15px; background-color:#FF0000; border:1px solid black;"></span> Conventional Hydrogen Bond | <span style="display:inline-block; width:15px; height:15px; background-color:#FF69B4; border:1px solid black;"></span> Pi-Pi T-shaped |
| <span style="display:inline-block; width:15px; height:15px; background-color:#00CED1; border:1px solid black;"></span> Halogen (Fluorine)         | <span style="display:inline-block; width:15px; height:15px; background-color:#DDA0DD; border:1px solid black;"></span> Pi-Alkyl       |

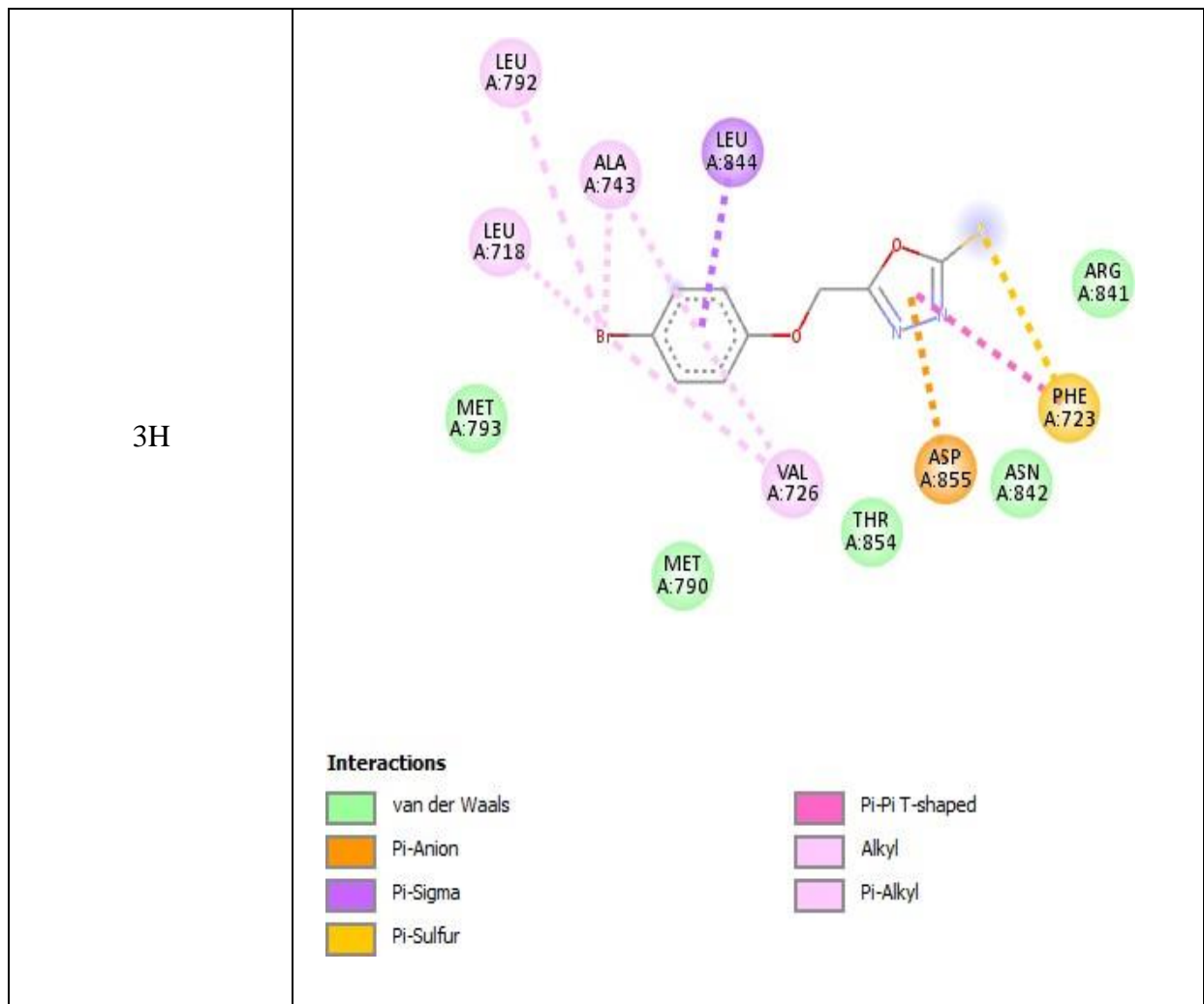
3E



**Interactions**

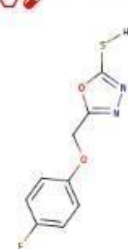
- |   |   |
|---|---|
| <span style="display:inline-block; width:15px; height:15px; background-color:#90EE90; border:1px solid black;"></span> van der Waals              | <span style="display:inline-block; width:15px; height:15px; background-color:#FF69B4; border:1px solid black;"></span> Pi-Pi T-shaped |
| <span style="display:inline-block; width:15px; height:15px; background-color:#FF0000; border:1px solid black;"></span> Conventional Hydrogen Bond | <span style="display:inline-block; width:15px; height:15px; background-color:#DDA0DD; border:1px solid black;"></span> Alkyl          |
| <span style="display:inline-block; width:15px; height:15px; background-color:#800080; border:1px solid black;"></span> Pi-Sigma                   | <span style="display:inline-block; width:15px; height:15px; background-color:#FFC0CB; border:1px solid black;"></span> Pi-Alkyl       |
| <span style="display:inline-block; width:15px; height:15px; background-color:#FFD700; border:1px solid black;"></span> Pi-Sulfur                  |   |






Hide BOILED-Egg model of Ligand-3D

**Molecule 1**
⊕



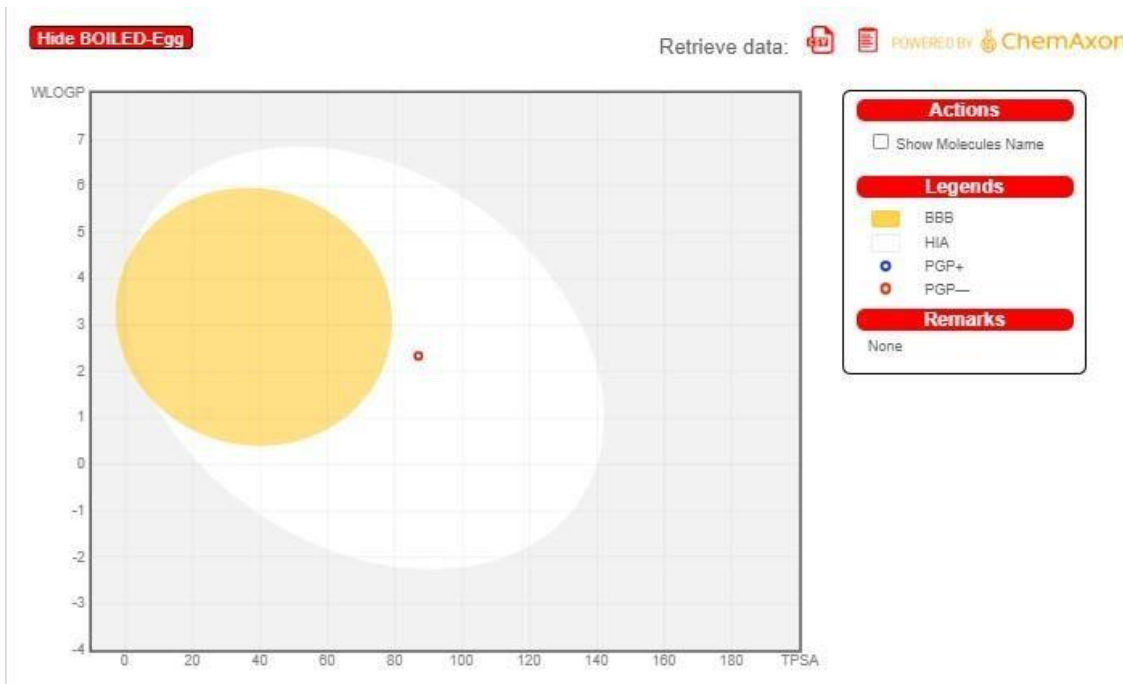
SMILES Fc1ccc(cc1)OCc1nnc(o1)S

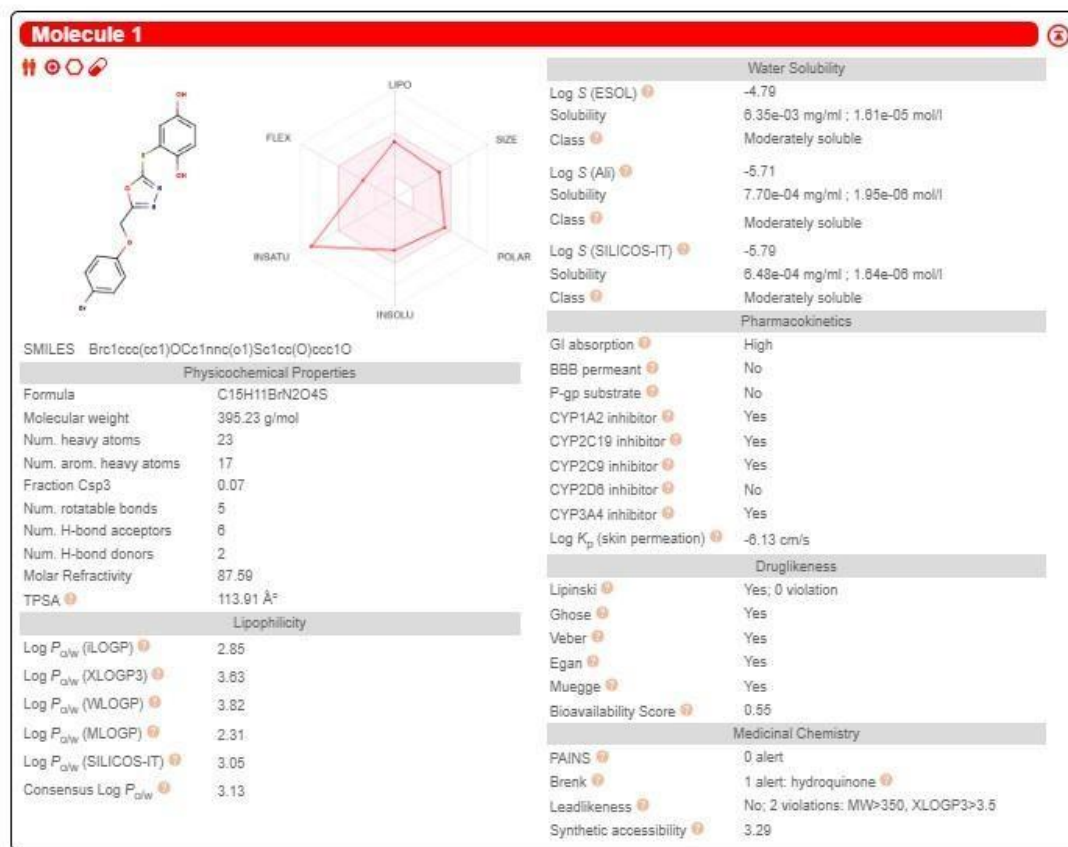


Water Solubility	
Log S (ESOL)	-2.75
Solubility	4.06e-01 mg/ml ; 1.79e-03 mol/l
Class	Soluble
Log S (Ali)	-3.29
Solubility	1.17e-01 mg/ml ; 5.17e-04 mol/l
Class	Soluble
Log S (SILICOS-IT)	-3.93
Solubility	2.68e-02 mg/ml ; 1.19e-04 mol/l
Class	Soluble
Pharmacokinetics	
GI absorption	High
BBB permeant	No
P-gp substrate	No
CYP1A2 inhibitor	Yes
CYP2C19 inhibitor	Yes
CYP2C9 inhibitor	No
CYP2D6 inhibitor	No
CYP3A4 inhibitor	No
Log K <sub>p</sub> (skin permeation)	-6.37 cm/s
Druglikeness	
Lipinski	Yes; 0 violation
Ghose	Yes
Veber	Yes
Egan	Yes
Muegge	Yes
Bioavailability Score	0.55
Medicinal Chemistry	
PAINS	0 alert
Brenk	1 alert: thio_2
Leadlikeness	No; 1 violation: MW<250
Synthetic accessibility	2.19

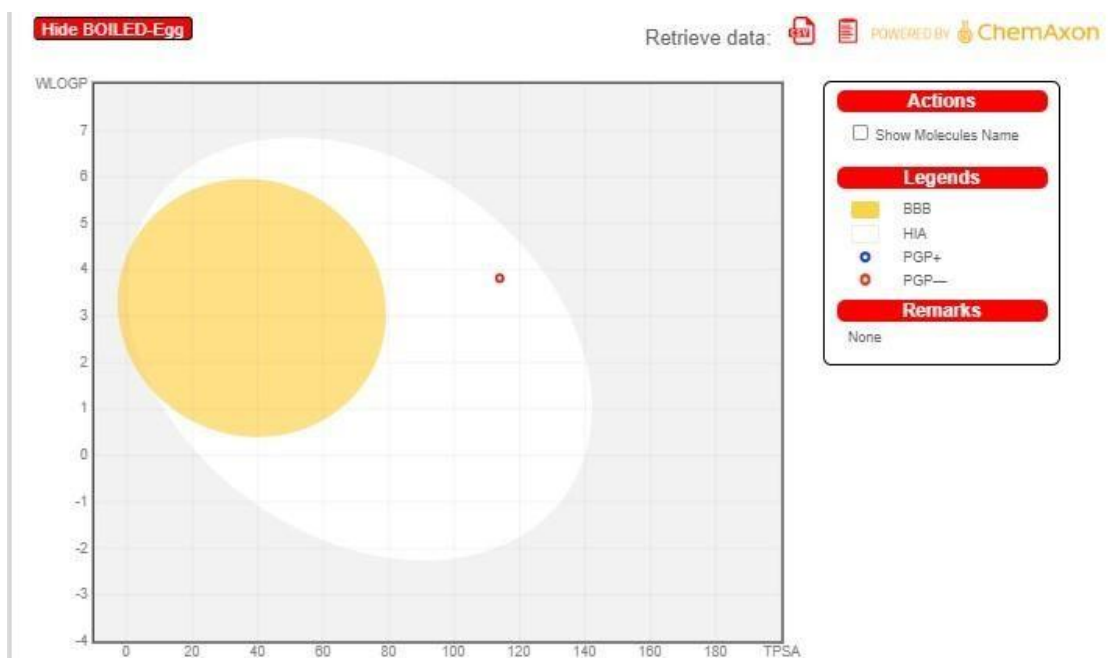
Physicochemical Properties	
Formula	C8H7FN2O2S
Molecular weight	226.23 g/mol
Num. heavy atoms	15
Num. arom. heavy atoms	11
Fraction Csp3	0.11
Num. rotatable bonds	3
Num. H-bond acceptors	5
Num. H-bond donors	0
Molar Refractivity	52.49
TPSA	86.95 Å <sup>2</sup>
Lipophilicity	
Log P <sub>ow</sub> (iLOGP)	2.38
Log P <sub>ow</sub> (XLOGP3)	1.84
Log P <sub>ow</sub> (WLOGP)	2.34
Log P <sub>ow</sub> (MLOGP)	1.50
Log P <sub>ow</sub> (SILICOS-IT)	2.44
Consensus Log P <sub>ow</sub>	2.10

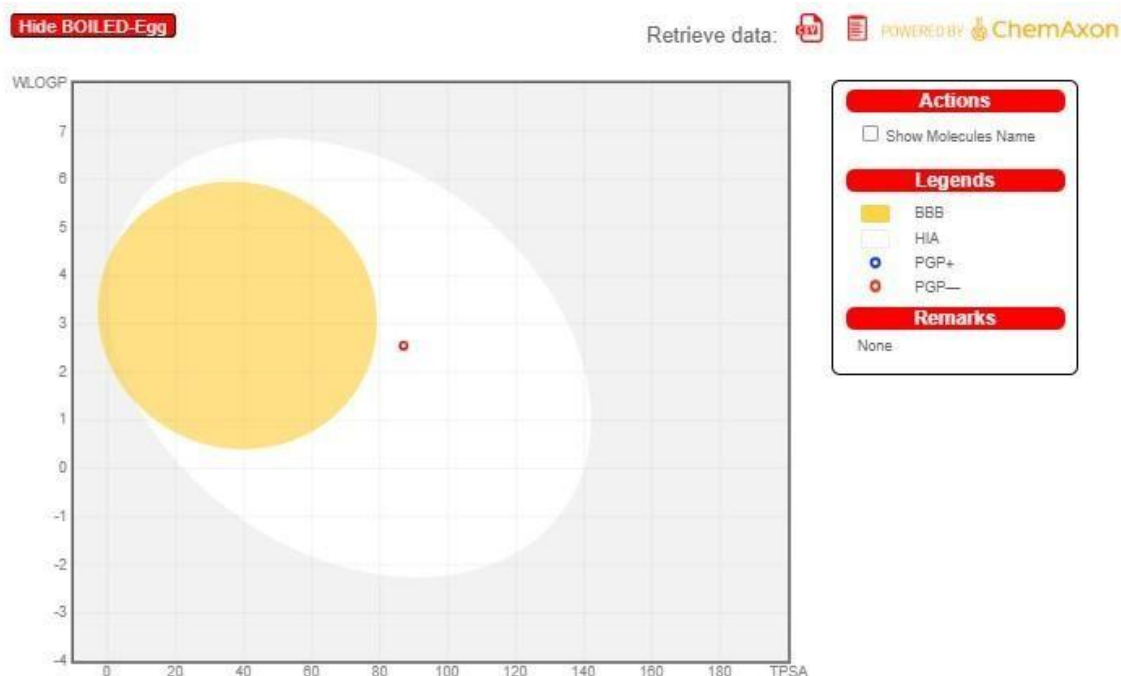
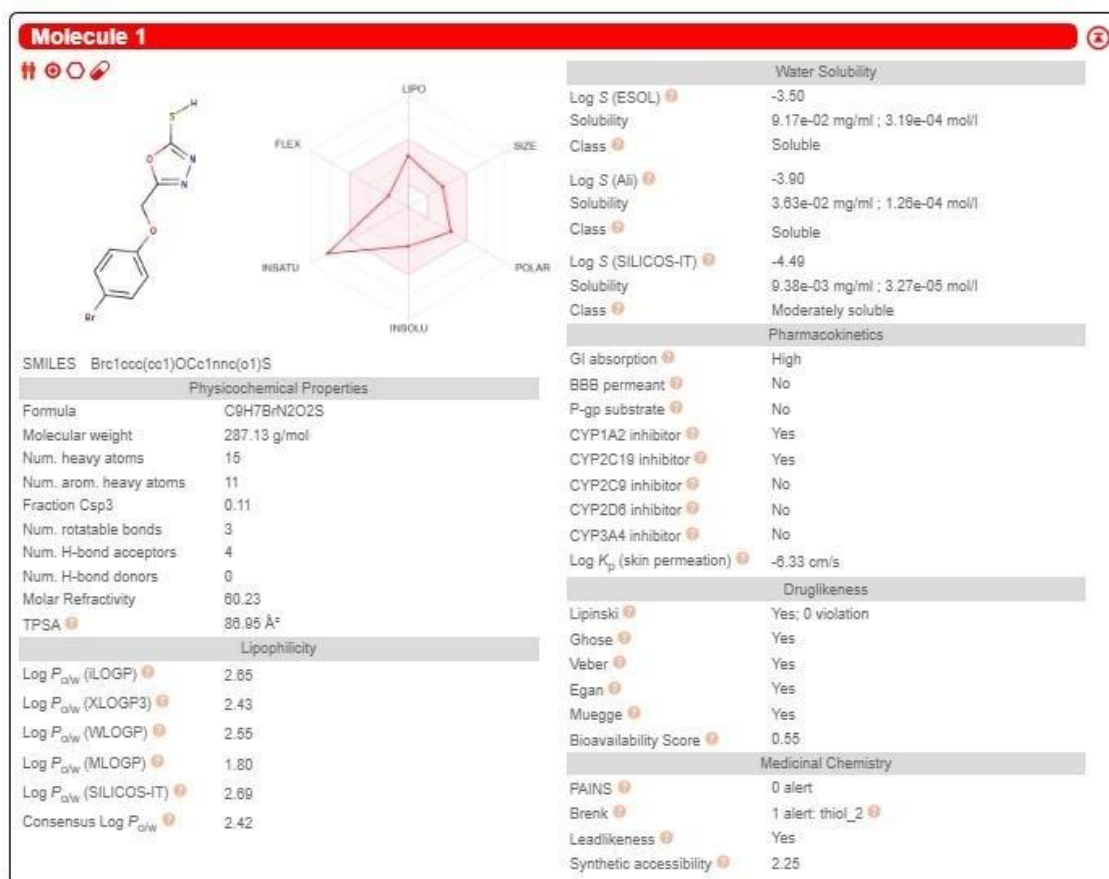
Hide BOILED-Egg model of Ligand-3E





Hide BOILED-Egg model of Ligand-3H





## Discussion

- The binding affinity is the strength of the interaction between two (or more than two) molecules that bind reversibly and show interactions.
- High-affinity ligand binding results from greater attractive forces between the ligand and its receptor while low-affinity ligand binding involves less attractive force.



- The ligands 3B,3A & 3C showed highest binding affinity with the values of -7.3,-7.2 and -7.2 respectively and rmsd values of 0 for all the compounds.
- The ligands E, F & G showed moderate binding affinity with the values of -7.0,-7.0 and -7.0 respectively and rmsd values of 0 for all the compounds.
- The ligands D and H showed low binding affinity with the values of -5.9 and -5.9 respectively and rmsd values of 0 for all the compounds.
- As depicted from Table-07, compound A makes one Hydrogen bonding interactions at the active site of the enzyme (PDB ID:6s9b), among those four interactions were of oxygen atom with hydrogen atoms of (THR A:854) and remaining oxygen atom of interactions with (LEU844, CYS797 and THR854).
- As depicted from Table-07, compound C makes no Hydrogen bonding interactions at the active site of the enzyme (PDB ID:6s9b), among those four interactions were of oxygen atoms of interactions with (THR854).
- As depicted from Table-07, compound D makes one Hydrogen bonding interactions at the active site of the enzyme (PDB ID:6s9b), among those four interactions were of oxygen atom with hydrogen atoms of (THR A:854) and remaining oxygen atom of interactions with (LEU844, CYS797 and THR854)
- As depicted from Table-07, compound G makes one Hydrogen bonding interactions at the active site of the enzyme (PDB ID:6s9b), among those four interactions were of oxygen atom with hydrogen atoms of (CYS797) and remaining oxygen atom of interactions with (ASP855 and CYS797).

#### Pharmacokinetics

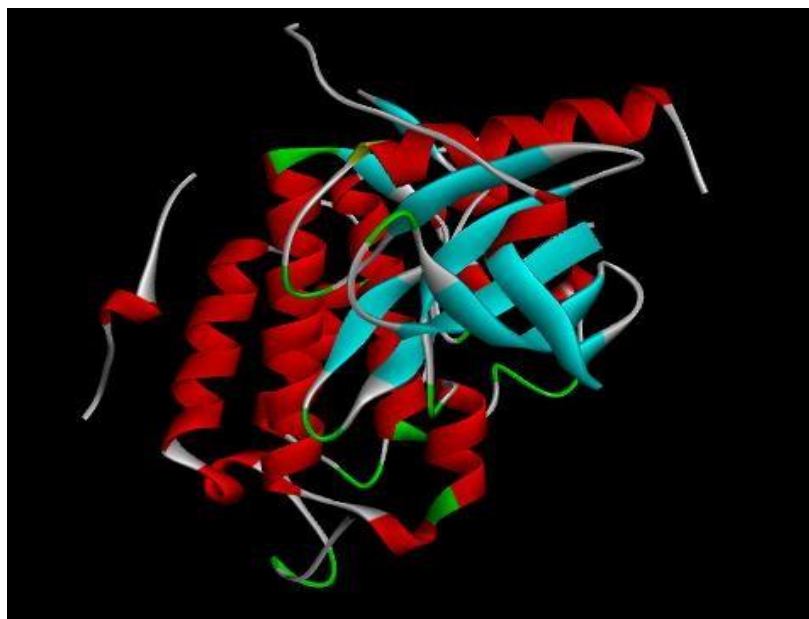
Among the docking ligands few ligands shown better pharmacokinetics and drug likeliness property

- The ligands 3A, 3B, 3C, 3D, 3E, 3F, 3G and 3H does not agree for BBB penetration, then, according to the yolk of boiled egg it does not obeys the pharmacokinetics of these ligands and predicts that the ligands are not druggable by this parameter.
- The P-gp substrate is not agreed for these ligands 3A, 3B, 3C, 3D, 3E, 3F, 3G and 3H and it is not expressed as BBB, hence does not allow the penetration of its substrates into the CNS.
- In GI absorption is (high) for these ligands, then, the white part of the boiled egg shows the high absorption of the ligands in the GI tract.
- Skin permeation: For the compounds 3A, 3B, 3C, 3D and 3H shows the values of -6.37 cm/s,-6.33 cm/s,-6.18 cm/s ,-6.18 cm/s and -6.18 cm/s which interpret high skin penetration property.

#### Drug Likeliness

- Lipinski filter: it is (yes) and 0 violation for the ligands 3A, 3B, 3C, 3D, 3E, 3F, 3G and 3H then it has molecular range less or equal to 500, so the compounds obey the drug likeliness properties.
- Lipinski's rule of five also known as the Pfizer's rule of five or simply the Rule of five (RO5) is a rule of thumb to evaluate drug likeness or determine if a chemical compound with a certain pharmacological or biological activity has properties that would make it a likely orally active drug in humans.
- Vebers rule: it is yes for these ligands, TPSA value is less than 140 and it obeys the drug likeliness properties.

- TPSA (Topological Polar Surface Area) it is used to measure the polar surface area that avoids the need to calculate ligand 3D structure or to decide which the relevant biological conformations is.



**Protein – 6s9b from PDB RCSB**

#### **4. Conclusion**

In summary, we have accomplished the docking study of newly synthesized derivatives of derivatives (3A-3H). Further, we have investigated their in-vitro antitubercular activity through MABA method. By performing docking studies, we got the results of ligand-receptor its binding affinity of the ligands, among which 3B, 3A and 3C showed higher binding affinity with the values of -7.3, -7.2 and -7.2. Compounds 3E, 3FG showed moderate binding affinity with the values of -7.0, -7.0 and -7.0 of the target active site of the enzyme 6s9b, the ligands A,B,C,D,E,F,G,H which showed zero violation for drug likeliness parameter that predicts these ligands obeys Lipinski rule and are less than 500 so they are druggable.

#### **5. References**

1. Nyarko RO, Prakash A, Kumar N, Saha P, Kumar R. Tuberculosis a globalized disease: Review. *Asian J Pharm Res Dev.* 2021;9(1):198–201.
2. Carranza C, Pedraza-Sanchez S, de Oyarzabal-Mendez E, Torres M. Diagnosis for Latent Tuberculosis Infection: New Alternatives. *Front Immunol.* 2020;11(S eptember):1–13.
3. Khan MT, Kaushik AC, Ji L, Malik SI, Ali S, Wei DQ. Artificial neural networks for prediction of tuberculosis disease. *Front Microbiol.* 2019;10(MAR):1–9.
4. Lekkala C, Bodala V, Yettula K, Karasala BK, Podugu RL, Vidavalur S. Copper-Catalyzed One-Pot Synthesis of 2,5-Disubstituted 1,3,4-Oxadiazoles from Arylacetic Acids and Hydrazides via Dual Oxidation. *ACS Omega.* 2022;7(31):27157–63.
5. Christof C, Nußbaumer-Streit B, Gartlehner G. WHO Guidelines on Tuberculosis Infection Prevention and Control. Vol. 82, *Gesundheitswesen.* 2020. 885-889 p.
6. AlMatar M, AlMandea H, Var I, Kayar B, Köksal F. New drugs for the treatment of

- Mycobacterium tuberculosis infection. *Biomed Pharmacother.* 2017;91:546–58.
7. Sia JK, Rengarajan J. Immunology of mycobacterium tuberculosis infections. *Gram-Positive Pathog.* 2019;1056–86.
  8. Kashid BB, Salunkhe PH, Dongare BB, More KR, Khedkar VM, Ghanwat AA. Synthesis of novel of 2, 5-disubstituted 1, 3, 4- oxadiazole derivatives and their in vitro anti-inflammatory, anti-oxidant evaluation, and molecular docking study. *Bioorganic Med Chem Lett* [Internet]. 2020;30(12):127136. Available from: <https://doi.org/10.1016/j.bmcl.2020.127136>
  9. Wang JJ, Sun W, Jia WD, Bian M, Yu LJ. Research progress on the synthesis and pharmacology of 1,3,4-oxadiazole and 1,2,4-oxadiazole derivatives: a mini review. *J Enzyme Inhib Med Chem* [Internet]. 2022;37(1):2304–19. Available from: <https://doi.org/10.1080/14756366.2022.2115036>
  10. Siwach A, Verma PK. Therapeutic potential of oxadiazole or furadiazole containing compounds. *BMC Chem* [Internet]. 2020;14(1):1–40. Available from: <https://doi.org/10.1186/s13065-020-00721-2>
  11. Atmaram UA, Roopan SM. Biological activity of oxadiazole and thiadiazole derivatives. *Appl Microbiol Biotechnol* [Internet]. 2022;106(9–10):3489–505. Available from: <https://doi.org/10.1007/s00253-022-11969-0>
  12. Mishra P, Rajak H, Mehta A. Synthesis of Schiff bases of 2-amino-5-aryl-1,3,4-oxadiazoles and their evaluation for antimicrobial activities. *J Gen Appl Microbiol.* 2005;51(2):133–41.
  13. Ahsan MJ, Samy JG, Khalilullah H, Nomani MS, Saraswat P, Gaur R, et al. Molecular properties prediction and synthesis of novel 1,3,4-oxadiazole analogues as potent antimicrobial and antitubercular agents. *Bioorganic Med Chem Lett* [Internet]. 2011;21(24):7246–50. Available from: <http://dx.doi.org/10.1016/j.bmcl.2011.10.057>
  14. Rajak H, Singour P, Kharya MD, Mishra P. A Novel Series of 2,5-Disubstituted 1,3,4-oxadiazoles: Synthesis and SAR Study for their Anticonvulsant Activity. *Chem Biol Drug Des.* 2011;77(2):152–8.
  15. Rajak H, Agarawal A, Parmar P, Thakur BS, Veerasamy R, Sharma PC, et al. 2,5-Disubstituted-1,3,4-oxadiazoles/thiadiazole as surface recognition moiety: Design and synthesis of novel hydroxamic acid based histone deacetylase inhibitors. *Bioorganic Med Chem Lett* [Internet]. 2011;21(19):5735–8. Available from: <http://dx.doi.org/10.1016/j.bmcl.2011.08.022>
  16. Ahsan MJ, Choupra A, Sharma RK, Jadav SS, Padmaja P, Hassan MZ, et al. Rationale Design, Synthesis, Cytotoxicity Evaluation, and Molecular Docking Studies of 1,3,4-oxadiazole Analogues. *Anticancer Agents Med Chem.* 2017;18(1):121–38.
  17. Ahsan MJ, Yadav RP, Saini S, Hassan MZ, Bakht MA, Jadav SS, et al. Synthesis, Cytotoxic Evaluation, and Molecular Docking Studies of New Oxadiazole Analogues. *Lett Org Chem.* 2017;15(1):49–56.
  18. Ahsan MJ, Shastri S, Yadav R, Hassan MZ, Bakht MA, Jadav SS, et al. Synthesis and Antiproliferative Activity of Some Quinoline and Oxadiazole Derivatives. *Org Chem Int.* 2016;2016:1–10.
  19. Ahsan MJ, Sharma J, Singh M, Jadav SS, Yasmin S. Synthesis and anticancer activity of n-aryl-5-substituted-1,3,4-oxadiazol-2-amine analogues. *Biomed Res Int.* 2014;2014.
  20. Salahuddin, Shaharyar M, Mazumder A, Ahsan MJ. Synthesis, characterization and anticancer evaluation of 2-(naphthalen-1-ylmethyl/naphthalen-2-ylloxymethyl)-1-[5-(substituted phenyl)-[1,3,4]oxadiazol-2-ylmethyl]-1H-benzimidazole. *Arab J Chem* [Internet]. 2014;7(4):418–24. Available from: <http://dx.doi.org/10.1016/j.arabjc.2013.02.001>
  21. Ningegowda R, Chandrashekarappa S, Singh V, Mohanlall V, Venugopala KN.

- Design, synthesis and characterization of novel 2-(2, 3-dichlorophenyl)-5-aryl-1,3,4-oxadiazole derivatives for their anti-tubercular activity against *Mycobacterium tuberculosis*. *Chem Data Collect* [Internet]. 2020;28:100431. Available from: <https://doi.org/10.1016/j.cdc.2020.100431>
22. Gan X, Hu D, Li P, Wu J, Chen X, Xue W, et al. Design, synthesis, antiviral activity and three-dimensional quantitative structure-activity relationship study of novel 1,4-pentadien-3-one derivatives containing the 1,3,4-oxadiazole moiety. *Pest Manag Sci.* 2016;72(3):534–43.
  23. Rabie AM. Two antioxidant 2,5-disubstituted-1,3,4-oxadiazoles (CoViTris2020 and ChloViD2020): Successful repurposing against COVID-19 as the first potent multitarget anti-SARS-CoV-2 drugs. *New J Chem.* 2021;45(2):761–71.
  24. Yatham S, Jadav SS, Gundla R, Gundla KP, Reddy GM, Ahsan MJ, et al. Design, Synthesis and Biological Evaluation of 2 (((5-aryl-1,2,4-oxadiazol-3-yl)methyl)thio)benzo[d]oxazoles: New Antiinflammatory and Antioxidant Agents. *ChemistrySelect.* 2018;3(37):10305–10.
  25. Rathore A, Sudhakar R, Ahsan MJ, Ali A, Subbarao N, Jadav SS, et al. In vivo anti-inflammatory activity and docking study of newly synthesized benzimidazole derivatives bearing oxadiazole and morpholine rings [Internet]. Vol. 70, *Bioorganic Chemistry.* 2017. 107-117 p. Available from: <http://dx.doi.org/10.1016/j.bioorg.2016.11.014>
  26. Kavitha S, Kannan K, Gnanavel S. Synthesis, characterization and biological evaluation of novel 2,5 substituted-1,3,4 oxadiazole derivatives. *Saudi Pharm J* [Internet]. 2017;25(3):337–45. Available from: <http://dx.doi.org/10.1016/j.jsps.2016.07.004>
  27. Lelyukh M, Martynets M, Kalytovska M, Drapak I, Harkov S, Chaban T, et al. Approaches for synthesis and chemical modification of non-condensed heterocyclic systems based on 1,3,4-oxadiazolering and their biological activity: A review. *J Appl Pharm Sci.* 2020;10(10):151–65.
  28. Akhter M, Husain A, Azad B, Ajmal M. Aroylpropionic acid based 2,5-disubstituted-1,3,4-oxadiazoles: Synthesis and their anti-inflammatory and analgesic activities. *Eur J Med Chem.* 2009;44(6):2372–8.